EXPLORING THE COMBINED USE OF DISTRIBUTED FIBER AND DEFORMED BAR REINFORCEMENT TO RESIST SHEAR FORCES

Quarterly Progress Report
For the period ending Nov 30, 2022

Submitted by:
PI: Travis Thonstad
Co-PI: Paolo Calvi
Research Assistant: John Paul Gaston

Affiliation: Department of Civil and Environmental Engineering
University of Washington

ACCELERATED BRIDGE CONSTRUCTION
UNIVERSITY TRANSPORTATION CENTER

Submitted to:
ABC-UTC
Florida International University
Miami, FL

1. Background and Introduction

Macro-synthetic fibers are often added to concrete mixtures as secondary reinforcement, designed to control shrinkage and temperature cracks and improve the durability of bridge superstructures. The addition of fibers to concrete improves the tensile behavior of the material, which leads to more durable concrete elements with increased ductility and better crack control. In addition to these desirable effects, the tensile strength of the fibers also contributes to the strength of the member, however this benefit is not included in current bridge design specifications [e.g., AASHTO 2020]. The lack of provisions regarding the use of macro-synthetic fibers as supplemental reinforcement is of detriment to the bridge construction industry because the use of fibers in PBEs and cast-in-place connections would result in a reduction of bar reinforcement and congestion, lighter members, smaller crack sizes, better distribution of localized stresses, and increased confinement and performance of member ends.

Developments in PFRCs are applicable to accelerated bridge construction (ABC) in two ways. The use of PFRC would permit thinner prefabricated bridge element (PBE) sections, enabling lighter members for transportation and erection. The great majority of ABC is conducted using PBEs, so any activity that benefits PBEs will encourage the use of them, and by direct implication, ABC. For prestressed girders, the use of PFRC could ameliorate the impacts of thinner girder webs by providing additional web-shear cracking strength, by arresting flexural cracks prior to their development into flexure-shear cracks, and by preventing splitting that would be exacerbated by the reduction in web width, as demonstrated in previous test series of girder end regions [e.g., Haroon et al. 2006]. The improved serviceability and durability of prestressed girders made from FRC would also create an additional incentive for owners to choose ABC techniques over other alternatives. Finally, the use of field-cast PFRC in ABC projects in connection regions would be beneficial by expediting on-site activities, alleviating congestion in connection regions and reducing the required deformed bar reinforcement.

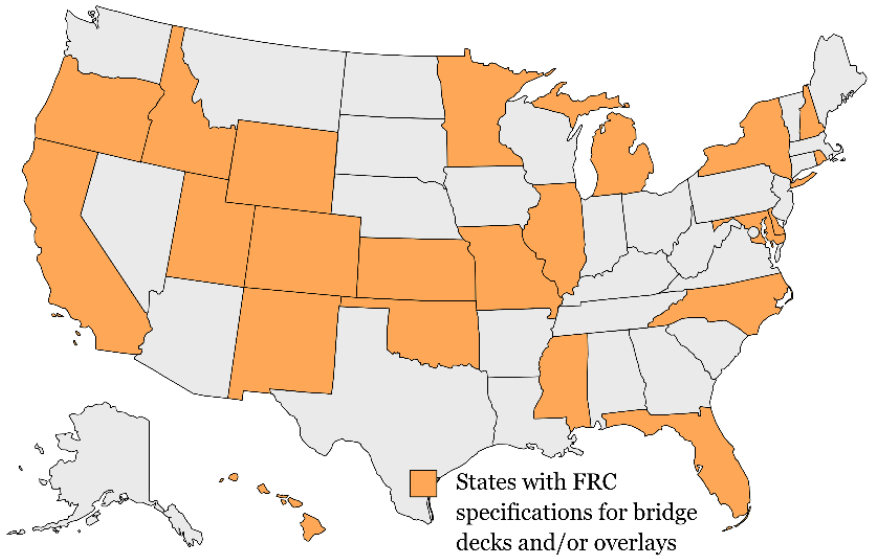

Fig. 1. States with FRC specifications for bridge decks and/or overlays, data from [Amirkhanian and Roesler 2019]

2. Problem Statement

Fiber-reinforced concrete already enjoys widespread use in practice, as shown in Fig. 1, and is required in several states (e.g., California, Oregon, and Delaware) for bridge decks [Amirkhanian and Roesler 2019]. The remaining bridge elements (e.g., prestressed girders) could similarly benefit from the improved strength and durability that FRC provides. To realize the full benefits of PFRC in practice, rational design equations are needed to predict the strength of members containing both macro-synthetic fibers and deformed bar reinforcement, particularly in shear. This research project will result in design guidelines for the combined use of distributed fiber and deformed bar reinforcement to resist shear forces, implementable in future bridge specifications.

3. Objectives and Research Approach

The objective of the proposed research is the development of simple, rational design equations for the contribution of macro-synthetic fibers to the shear strength of reinforced concrete members containing at least the minimum shear reinforcement required by the *AASHTO LRFD Bridge Design Specifications* [AASHTO 2020]. The design equations will be based on a rational shear behavior model that will be developed as part of this work using the response of PFRC panel elements, subjected to in-plane loads (e.g., shear and axial tension or compression). The PI's are uniquely positioned to develop a shear behavior model for PFRC members due to the experimental capabilities available at the University of Washington's (UW) Large-Scale Structural Engineering Testing Laboratory (SETL) and the ability to generate uniform shear stress states using the UW SETL Panel Element Tester. A similar experimental apparatus was used to develop the Modified Compression Field Theory [Vecchio and Collins 1986], which is the basis for the current shear provisions in the *AASHTO LRFD Bridge Design Specifications*. Thus, the experimental data collected will be uniquely suitable for developing the proposed design equations.

4. Description of Research Project Tasks

The following is a description of tasks carried out to date.

Task 1 – Literature Review

This task is complete. The objective of this task was to establish a database to be used to evaluate the design expression developed in Task 3. An extensive review of past experimental research involving polyolefin fiber-reinforced concrete was completed, focusing on specimens that utilized both deformed bar and fiber reinforcement to resist shear forces. The collected data is summarized in Table 1.

Table 1. Structural testing of polyolefin fiber-reinforced concrete members with and without conventional deformed bar reinforcement

Author	Test	Specimen	Fiber Length (mm)	Fiber Aspect Ratio	Fiber Modulus (GPa)	Fiber Geometry	Fiber volume	Conventional reinforcement	Key conclusions
Li et al. 1992	Flexure/ Shear	Beams	12.7	334	100	Straight	V_f = 1.0%	ρ_ℓ = 1.1% / 2.2% ρ_v = 0%	Strength increased between 100-200% when a 1% volume fraction of fibers was used. Possible to obtain ductile flextural failures for variety of reinforcement and span-to-depth ratios.
Li et al. 1994	Shear	Ohno shear beams	12.7	334	100	Straight	V_f = 2.0%	ρ_ℓ = 0% / 0.75% ρ_v = 0% / 0.75%	Fiber reinforced beam exhibted higher shear strenth than plain concrete specimen and lower strength than reinforced one Fibers did not improve first cracking load. Fiber reinforced specimen had improved ultimate strain over beam with conventional concrete and welded wire fabric reinforcement.
Furlan and Bento de Hanai 1997	Flexure/ Shear	Beams	42	840		Multi-filament	V_f = 0% / 0.50%	ρ_ℓ = 1.58% ρ_v = 0.18%	Addition of fibers increased stiffness, improved ductility, increased the shear strength, and led to the formation of multiple cracks at failure in the beams Addition of fibers modified the failure mode of the beams from shear to flexure in the presence of stirrups.
Majdzadeh et al. 2006	Flexure/ Shear	Beams	50 54	85 360	9.5 3.5	Straight Self-fibrillating	V_f = 0% / 0.5% / 1.0% / 1.5%	ρ_ℓ = 2.62% ρ_v = 0% / 0.14%	Fiber reinforcement enhanced the capacity of the beams. No benefits were noted when the volume fraction was increased beyond 1%. Beams with both stirrups and fibers had higher strengths than beams containing only stirrups, and the increase was larger than expected given the resistance of the beams tested with only fibers or stirrups alone.
Roesler et al. 2006	Out-of-plane shear	Slabs on grade	40	90	9.5	Straight	V_f = 0% / 0.32% / 0.48%	ρ_ℓ = 0% ρ_v = 0%	Flexural cracking load and strength increased by roughly 30% with addition of fibers The fibers did not increase the tensile capacity of the concrete slabs. Instead, a larger percentatge of the fiber reinforced concrete slabs remained in contact with the ground throughout testing, leading to improved capacity.
Altoubat et al. 2009	Flexure/ Shear	Beams	40	90	9.5	Straight	V_f = 0% / 0.5% / 0.75% / 1.0%	ρ_ℓ = 2.15% / 3.18% ρ_v = 0%	Addition of fibers increased first diagonal cracking strength and ultimate strength roughly of 20-30% Beam response with fibers was more ductile than control RC beams Fibers changed the cracking pattern and mode of failure of the beams. The fiber-reinforced beams exhibited multiple diagonal cracks before failure occurred. Fibers did not change the load at which the diagonal cracks initiated but did slow down propagation and widening

Author	Test	Specimen	Fiber Length (mm)	Fiber Aspect Ratio	Fiber Modulus (GPa)	Fiber Geometry	Fiber volume	Conventional reinforcement	Key conclusions
Cornovale and Vecchio 2014	Shear	Panel element	54	67	10	Crimped	V_f = 0% / 2.0%	ρ_ℓ = 3.31% ρ_v = 0% / 0.42%	First cracking of PFRC panels was accompanied by a sharp drop in load and development of large crack widths Addition of fibers improved ductility, polyolefin fibers can transmit relatively high tensile stress across crack widths No degradation in properties under cyclic loads was observed for macro-synthetic fiber-reinforced panels
Altoubat et al. 2016	In-plane shear	Composite slabs	40	90	9.5	Straight	V_f = 0% / 0.32% / 0.58%	ρ_ℓ = 0% ρ_v = 0%	Secondary reinforcement (wire mesh, fibers) has no effect on interfacial bond with decking Fiber reinforced slab panels exhibited multiple cracks before failure Fibers and wire mesh provided similar improvements to the ductility and post-peak behavior of specimens Addition of 0.58% macro-synthetic fibers led to 20%-40% increase in ultimate load capacity versus the unreinforced specimens
Alhassan et al. 2017	Flexure/ Shear	Beams	40	90	9.5	Straight	V_f = 0% / 0.33% / 0.55% / 0.77%	ρ_ℓ = 1.26% / 1.81% / 2.46% / 3.22% ρ_v = 3.33%	Slight increase in strength: roughly 20% increase in strength for a fiber volume fraction of 0.77% Initial, service, and post-cracking stiffness increased with fiber volume fraction
Ortiz-Navas et al. 2018	Shear friction	Push off (pre-cracked)	48	57	4.7	Crimped	V_f = 0% / 1.1% /	ρ_{vf} = 0%, 0.16%	Initial crack opening influenced stiffness and strength of fiber reinforced specimens less than unreinforced ones Addition of fibers increased shear and normal stresses transferred across the crack
Patil et al. 2020	Flexure/ Shear	Columns	50	100	10	Deformed	V_f = 0% / 0.35% / 0.7% / 1.0%	ρ_ℓ = 0.84% GFRP ρ_v = 0.35% GFRP	Addition of fibers improved post-cracking stiffness of beams Fibers caused a marginal increase in peak strength

Task 2 – Panel testing program

This task is ongoing. The objective of this task was to elucidate the contributions and benefits of the separate and combined used of deformed bar and macro-synthetic fiber reinforcement. Previous tests of PFRC members did not include deformed bar reinforcement or included only a single deformed bar reinforcement configuration ($\rho_v \approx 0.15\%$ for both test series). This was one of the first experimental programs to specifically investigate the interaction between macro-synthetic fibers and deformed bar reinforcement in resisting shear forces and provides valuable data that is needed to build a shear behavior model in Task 3.

Table 2 shows the test matrix for the panel testing program and progress to date. The variables of interest within the experimental campaign include the deformed bar and macro-synthetic fiber reinforcement ratios, expressed as V_f the fiber volume fraction (fiber volume / total volume), and ρ_v the transverse reinforcement ratio (area of deformed bar / thickness of element × bar spacing). To ensure that shear failure occurred in the y-direction, the reinforcement ratio in the x-direction was set at $\rho_x = 2.28\%$. A 3×4 full factorial experimental design was selected to enable the quantification of interactions between the primary variables and ample coverage of the region of interest. The selected fiber volume fractions were consistent with what is currently used in practice.

Table 2. Panel test matrix and progress to date

Panel	V_f (%)	ρ_v (%)	Status
PFRC-000-000	0	0	TESTED
PFRC-000-029	0	0.29	TESTED
PFRC-000-058	0	0.58	TESTED
PFRC-000-114	0	1.14	
PFRC-026-000	0.26	0	TESTED
PFRC-026-029	0.26	0.29	
PFRC-026-058	0.26	0.58	TESTED
PFRC-026-114	0.26	1.14	
PFRC-052-000	0.52	0	TESTED
PFRC-052-029	0.52	0.29	CONSTRUCTED
PFRC-052-058	0.52	0.58	TESTED
PFRC-052-114	0.52	1.14	

Fig. 2 shows the selected reinforcement layouts for the panel specimens. All reinforcement for the project was No. 3 A706 Gr 60 from the same heat. For all configurations, the longitudinal reinforcement ratio was held constant at $\rho_t = 2.28\%$. This reinforcement ratio was selected to force failure in the transverse direction and was based on previous experience with similarly reinforced specimens tested with the panel tester [e.g., Zhang et al. 2020]. In the transverse direction, the spacing of the continuous reinforcement varied between panels, from $\rho_y = 0.29\%$ to $\rho_y = 1.14\%$, with three unreinforced specimens ($\rho_y = 0\%$) acting as benchmarks.

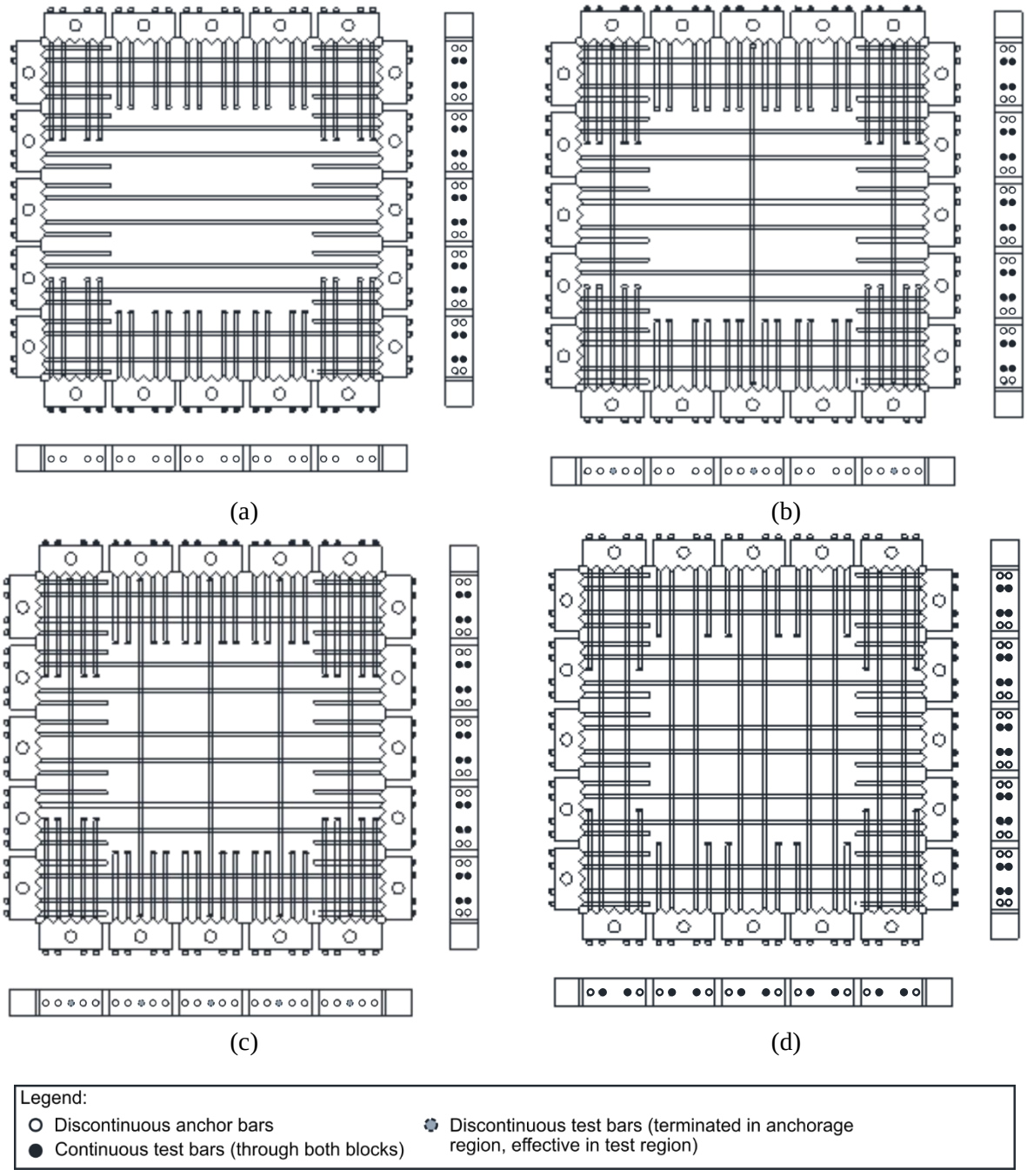

Fig. 2. Reinforcement layout for panel specimens with ρ_ℓ = 2.28% for all configurations (a) ρ_y = 0% [P1, P5, P9], (b) ρ_y = 0.29% [P2, P6, P10], (c) ρ_y = 0.58% [P3, P7, P11], (d) ρ_y = 1.14% [P4, P8, P12]

All experiments were conducted at the UW SETL. The panel specimens were tested using the UW SETL Panel Element Tester, shown in Fig. 3. The Panel Element Tester is an advanced apparatus that can apply any combination of in-plane stresses. The predetermined stress state is applied using 37 hydraulic actuators with 8 in. stroke. The panel specimens, roughly 36 in x 36 in x 3 in, were connected to the actuators through rigid links attached to steel "toothed" anchor blocks affixed to

the concrete panel. Each deformed bar embedded in the panel concrete was threaded at its ends, passed through the steel anchor blocks, and anchored to the blocks using nuts. The force from the actuators was resisted by a stiff reaction frame. Load cells and pressure transducers were used to control forces and pressures that develop in the actuators. The deformations in the panels were monitored using non-contact instrumentation and affixed displacement transducers.

Fig.3. UW SETL Panel Element Tester setup

Table 3 gives the concrete mixture proportions for the panel specimens. To accommodate wetting the surface area of the macro-synthetic fibers, the mixture design without fibers (M1) for panels 1-4 was modified by replacing three fiber volumes of fine aggregate with one fiber volume of fibers and two fiber volumes of coarse aggregates (M2 for panels 5-8 and M3 for panels 9-12). The original mixture design was selected in coordination with CalPortland, a regional ready mixed concrete supplier, who donated the aggregate from their aggregate plant in Dupont, WA. The fine aggregate was AASHTO M 6, washed building sand, and the coarse aggregate was AASHTO No 8, washed 3/8 in pea gravel. Selecting a commercially available concrete mixture and procuring aggregate from their plant was advantageous to ensure that the research results were consistent. Building on the current project, larger batches of this commercially available concrete mixture can then later be procured with similar properties for future tests of beams and connection specimens, planned as follow-on studies to this one.

Table 4 gives the properties of the macro-synthetic fibers that were used for the panel specimens (STRUX 90/40). The fibers used in this experimental program were from the same lot, are straight, and have a rectangular cross-section. A schematic of the fibers is shown in Fig. 4. These fibers were selected due to their high modulus and successful use in a number of previous tests of structural members. GCP Applied Technologies donated the fibers and concrete admixtures that were used for the project. The fibers comply with ASTM D7508 [ASTM 2020b] and have been evaluated by the ICC (ESR-2942).

Table 3. Concrete mixture design for panel specimens

	Absorp (%)	Specific Gravity	**M1:** 0% Fiber*	**M2:** 0.25 % Fibers*	**M3:** 0.52% Fibers*
			Mass [Volume] (lb [ft^3])		
Cement		3.15	534 [2.72]	534 [2.72]	534 [2.72]
Fine Aggregate	2.10	2.65	1447 [8.75]	1413 [8.55]	1380 [8.34]
Coarse Aggregate	1.12	2.68	1815 [10.85]	1838 [11.06]	1860 [11.12]
Water			267 [4.28]	267 [4.28]	267 [4.28]
Air (1.5%)			0 [0.41]	0 [0.41]	0 [0.41]
Fibers		0.92	0	4 [0.07]	8 [0.13]
Total			4062 [27.00]	4059 [27.00]	4056 [27.00]

* Includes WRDA64, ADVA195, VMAR3 at dosage rates in the range of 3-25 fl. oz / yd^3

Table 4. Fiber properties for panel specimens

Property	Value
Material	100% Virgin polypropylene and polyethylene blend
Specific gravity	0.92
Modulus of elasticity	1,389 ksi (9.5 GPa)
Tensile strength	90 ksi (620 MPa)
Nominal Length	1.55 in. (40 mm)
Nominal Width	0.055 in (1.4 mm)
Nominal Thickness	0.004 in (0.105 mm)
Nominal Equivalent Diameter	0.017 in (0.43 mm)
Nominal Aspect Ratio	90 (based on equivalent diameter)
Nominal Fiber Count	85,100 per lb (187,000 per kg)

Fig. 4. STRUX 90/40 fiber dimensions

The construction sequence for the panels is summarized in Fig. 5. First, the casting table was oiled, and the anchor blocks were installed (see Fig. 5a). Next, the threaded rebar was slid through the anchor blocks, tied together, and fastened to the anchor blocks with a combination of standard and jam nuts (see Fig. 5b). The gaps between the blocks and between the rebar and blocks were filled with plasticine to prevent leaks during casting. The slump was tested, and then the concrete was placed into the steel panel element form, around the reinforcement using hand scoops, in two lifts, as shown in Fig. 5c. The first lift filled the panel to roughly the level of the first layer of reinforcement, and the second lift filled the remainder of the panel. This procedure attempted to minimize the number of fibers that draped over the reinforcement during concrete placement. The panel elements were consolidated using a pneumatic external vibration bolted to the bottom of the casting table. Additionally, the corners and edges of the panel were consolidated using internal

vibration, performed approximately 1-2 inches from the edges of the panel every 4-6 inches, using a 1-1/2 HP vibrator with a 1 in diameter head. The specimens were given a smooth finish and remained on the casting table for a minimum of 3 days prior to lifting the panel (see Fig. 5d). The specimens remained covered with wet burlap and plastic sheeting for at least 7 days.

Fig. 5. Construction sequence (a) bare casting table and anchor blocks, (b) tied reinforcement cage prior to casting (c) consolidation of panel specimen (d) specimen curing under wet burlap/plastic

After 7 days, the specimens were air cured for at least an additional 21 days prior to testing. Throughout the curing process, the RH and temperature of the laboratory, where the specimens were stored, was monitored and recorded.

To accompany the panel elements, 4×8 cylinders and ASTM C1609 [ASTM 2020c] beams were cast at the same time as the panel elements. These companion specimens were used to determine strength and toughness parameters needed to develop the shear behavior model in Task 3. At minimum, cylinders were tested prior to lifting the panels, at 28 days, and the day of the panel tests. Beams were tested on the day of the panel element test. The curing conditions for the companion specimens matched that of the panels. The specimens remained in their molds under wet burlap for a minimum of 7 days, then were demolded and allowed to air cure adjacent to the panel in the laboratory. Table 5 gives a summary of the measured material properties on testing day for the three concrete mixes.

Table 5 Test day mechanical properties of companion cylinders and flexure beams

Panel	Specimen name	Flexure, 4×4 beams	Flexure, 6×6 beams

		Compressive strength (psi)	Elastic modulus (ksi)	Peak, f_1 (psi)	Residual, f_{150} (psi)	Peak, f_1 (psi)	Residual, f_{150} (psi)
P1	PFRC-000-000	6400	4700	750			
P2	PFRC-000-029	5500	4100	850			
P3	PFRC-000-058	4500	4300	440			
P4	PFRC-000-114						
P5	PFRC-026-000	4700	3800	720	70	860	100
P6	PFRC-026-029						
P7	PFRC-026-058	5000	3900	780	60	700	90
P8	PFRC-026-114						
P9	PFRC-052-000	4100	*	590	140	530	170
P10	PFRC-052-029						
P11	PFRC-052-058	5100	4700	560	130	630	110
P12	PFRC-052-114						

* Not available due to an instrument malfunction during testing

Testing has been progressing in the lab with over half of the specimens constructed and tested. The data has been validated and minimally processed thus far, with the graduate student focusing instead on the ongoing laboratory work. Data from the first two reference panels (without fiber reinforcement) has been analyzed, however, and is presented here

Testing of the first reference panel (no transverse reinforcement or fibers) has been completed. Fig. 6 summarizes the results of the first test. Shear stresses were applied to the panel through the steel “toothed” anchor blocks. The applied shear stresses were measured using pressure transducers attached to the hydraulic system. Shear stress was slowly incremented, and balanced, between the actuators using a mechanical load maintainer. The deformation of the panel was monitored using non-contact instrumentation system (see Fig. 6c) and affixed displacement transducers (see Fig. 6a).

A preliminary plot of the shear stress-strain behavior for the panel is shown in Fig. 6b. Shear stress was applied to the panel until first cracking, at which point visually identifiable shear cracks formed, roughly 0.5 mm in width. The loading was paused, and photographs were taken of the observed damage. Because the specimen was unreinforced in the test region, localization and failure occurred promptly after this brief pause for photographs and never reached a strength greater than the load to cause first cracking. Beyond this point, the deformations localized at a single diagonal crack in the panel (which aligns with the longitudinal reinforcement in the x-direction) and the two halves of the specimen translated relative to one another as essentially rigid bodies (see Fig. 6d). The ultimate strength of panel P1 was 2.12 MPa. For comparison, the unreinforced panel tested by Zhang et al. 2020, which contained 50% recycled aggregate, was 2.01 Mpa.

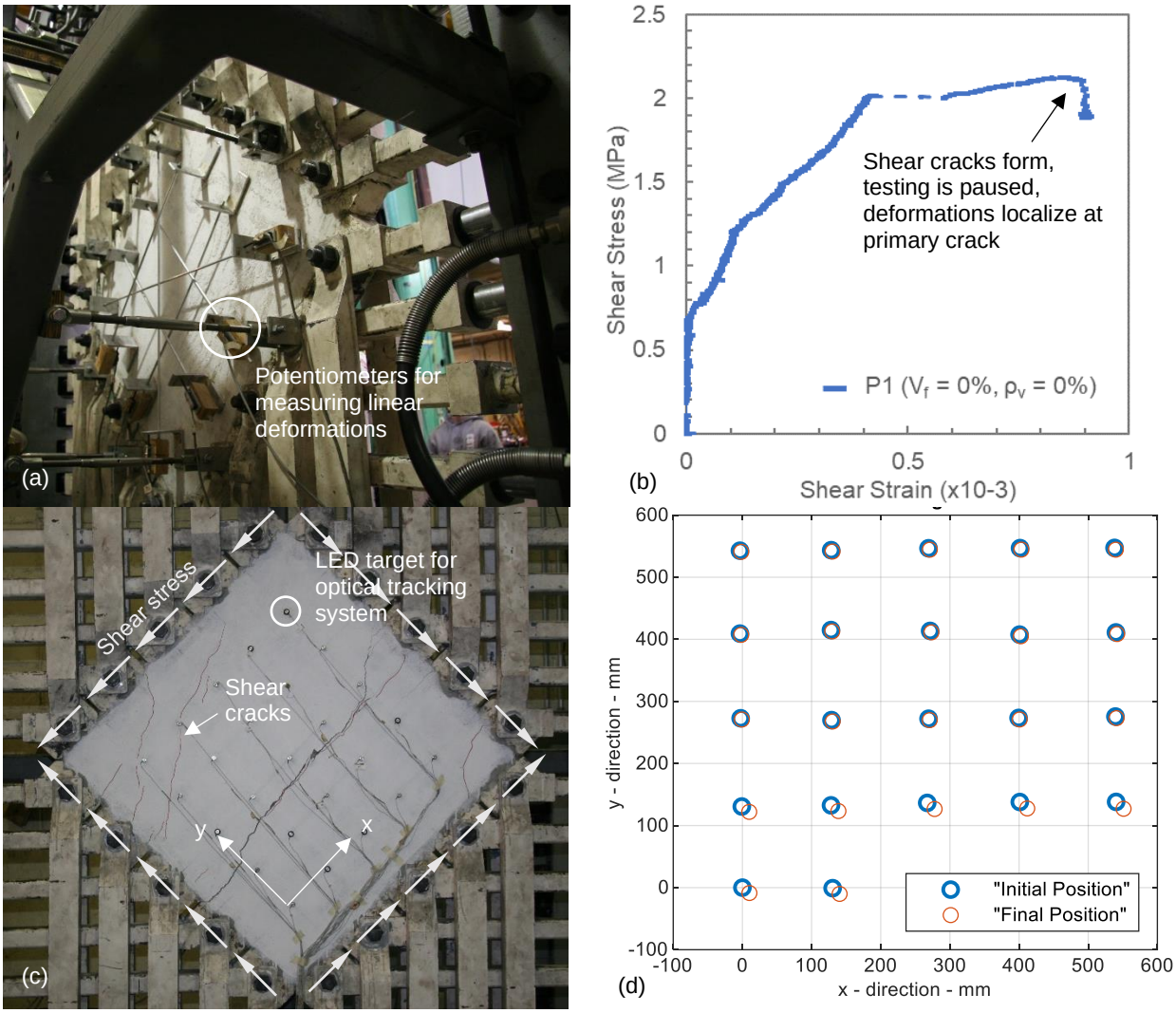

Fig. 6. Panel 1 test summary (a) potentiometer configuration and out-of-plane bracing, (b) preliminary shear stress-strain behavior (c) cracking pattern at failure (d) LED target locations and displacements during testing

Testing of the second reference panel (with 0.58% transverse reinforcement and without fibers) has also been completed. Shear stress was applied to the panel until first cracking, at which point visually identifiable shear cracks formed, roughly 0.5 mm in width. The loading was paused, and photographs were taken of the observed damage. The load was then increased in increments, pausing after each increment to document cracking, starting at a shear stress of 300 psi and continuing in 100 psi increments until failure. The data has been processed and validated, allowing the research team to compare the results of the present study with those from previous testing campaigns that used the same testing apparatus.

Fig. 7 compares the normalized shear stress-strain behavior (normalized by the test-day compressive strength of companion cylinders) for the two reference panels with three panels tested by Zhang et al. (2020). The results generally follow similar trends and the normalized strengths are consistent, considering the transverse reinforcement ratios used in each of the panel specimens.

This result gives confidence that the panel tester is operating as intended and the data is of good quality.

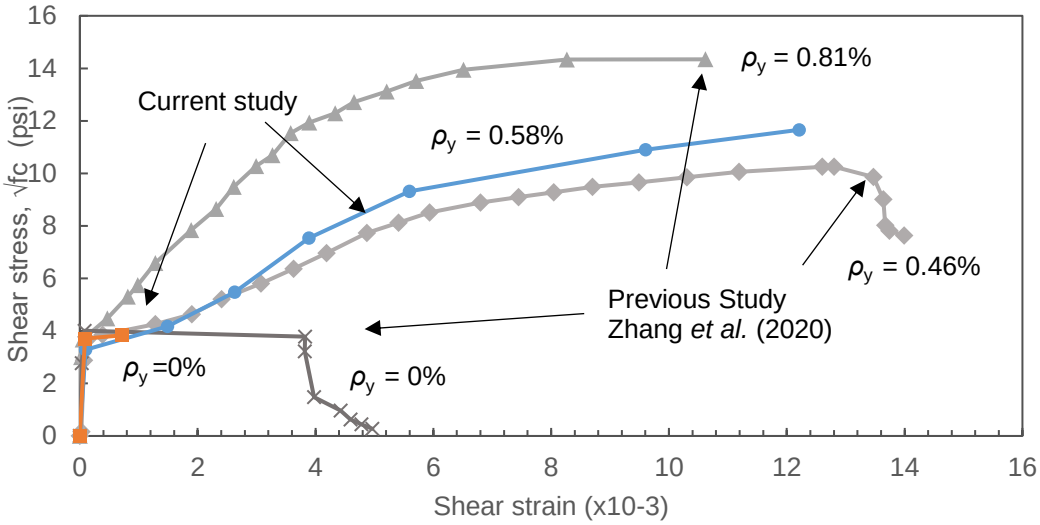

Fig. 7. Normalized shear stress-strain behavior for reference panels

Fig. 8 shows the crack pattern and crack widths for the second reference panel at a shear stress value of 500 psi, corresponding to a normalized shear stress of $7.5\sqrt{f_c}$. At this stress level, the maximum crack width in the test region was 0.3 mm, and the average crack width was 0.24 mm, determined through visual inspection and crack comparator. The cracks are oriented vertically, aligned with the principal tension direction, as would be expected given the imposed shear stresses. The manual crack maps have been manually digitized for each load increment.

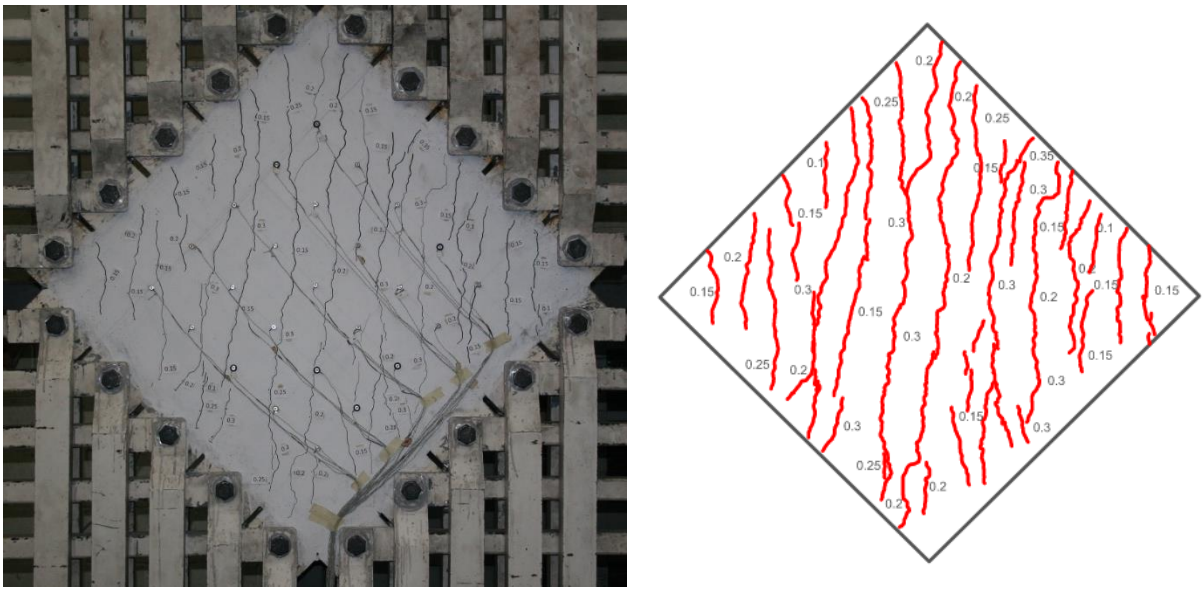

Fig. 8. Crack pattern and crack widths (in mm) for PFRC-000-058 at 500 psi shear stress $(7.5\sqrt{f_c})$

To date, seven panel specimens have been tested. A detailed analysis of the behavior of the fiber reinforced panels, in the context of the other panel specimens remaining to be constructed and tested, will be presented in future reports.

Task 3 – Development of design recommendations

This task has not yet started. The results of the panel tests in Task 2, will be used to develop rational design recommendations that capture the potential beneficial interaction between deformed bar and distributed fiber reinforcement. These equations would add to, or modify, the steel contribution of the elements shear strength based on the interactions measured during the experimental testing program (Task 2).

Although the existing literature on fiber reinforced concrete beams includes numerous proposed equations for the fiber contribution to shear strength, these equations were developed using databases of SFRC beams without stirrups and are therefore likely unsuitable for elements that contain both deformed bar and distributed macro-synthetic fiber reinforcement. However, both the newly developed code-oriented equations and those existing empirical relationships from the literature will be evaluated against the test data available for beams containing both fibers and deformed bar reinforcement gathered during Task 1.

The design recommendations will be established in cooperation with the advisory panel and industry professionals to develop language suitable for submission to AASHTO T10 Committee for adoption.

Task 5 – Interim and Final Reporting

This task in ongoing. The research team will submit timely quarterly reports, present annually at the Research Days meeting, and complete a final report summarizing findings reached during the project.

5. Expected Results and Specific Deliverables

The successful completion of the research project will directly impact the design/construction industry, by providing guidelines for the combined use of distributed fibers and deformed bars to resist shear in field-cast and precast reinforced concrete bridge elements and connections, quantifying the potentially beneficial interaction between the two types of reinforcement.

The expected products resulting from this research will include:

- Database of structural tests of fiber reinforced concrete elements that also contained deformed bars for shear reinforcement,
- Recommended guidelines for the sectional shear strength of PFRC elements with at least the minimum deformed bar shear reinforcement, and
- Design example that demonstrates new design equations.

In addition, the results of the project will be summarized in a 5-min demonstration video and a journal publication.

6. Schedule

Progress on tasks in this project is shown in the tables below.

Item	% Completed
Percentage of Completion of this project to Date	40%

Research Tasks	2022							2023							
	J	J	A	S	O	N	D	J	F	M	A	M	J	J	A
Task 1 – Literature Review															
Task 2 – Panel Testing Program															
Task 3 – Development of Design Recommendations															
Task 4 – Interim and Final Reporting															

7. References

AASHTO (2020) *AASHTO LRFD Bridge Design Specifications (9th Edition)*. American Association of State Highway and Transportation Officials (AASHTO), Washington, DC.

Alhassan, M., Al-Rousan, R., Ababneh, A. (2017) "Flexural behavior of lightwight concrete beams encompassing various dosages of macro synthetic fibers and steel ratios." *Case Studies in Constr Mat*, 7: 280-293.

Altoubat, S., Yazdanbakhsh, A., and Rieder, K.A. (2009). Shear behavior of macro-synthetic fiber-reinforced concrete beams without stirrups. *ACI Mat J*, 106(4): 381-389.

Altoubat, S., Ousmane, H., Barakat, S. (2016) "Experimental Study of In-Plane Shear Behavior of Fiber-Reinforced Concrete Composite Slabs." *J Struct Eng*, 142(3): 04015156

Amirkhanian, A. and Roesler, J. (2019) "Overview of Fiber-Reinforced Concrete Bridge Decks." InTrans Report 15-532, Iowa State University, Ames, IA

ASTM (2020a) "ASTM C192-19: Standard Practice for Making and Curing Concrete Test Specimens in the Laboratory," ASTM International.

ASTM (2020b) "ASTM D7508-20: Standard Specification for Polyolefin Chopped Strands for Use in Concrete," ASTM International.

ASTM (2020c) "ASTM C1609-19: Standard Test Method for Flexural Performance of Fiber-Reinforced Concrete (Using Beam With Third-Point Loading)," ASTM International

Carnovale, D. and Vecchio, F.J. (2014). Effect of Fiber Material and Loading History on Shear Behavior of Fiber-Reinforced Concrete. ACI Struct J, 111(5): 1235-1244.

Furlan, S. and Bento-de-Hanai, J.B. (1997). Shear behavior of fiber reinforced concrete beams. Cement and Concrete Composites, 19: 359–366.

Haroon, S., Yazdani, N., and Tawfiq, K. (2006) "Posttensioned Anchorage Zone Enhancement with Fiber-Reinforced Concrete." J Bridge Eng, 11(5): 566-572.

Lantsoght, E.O.L. (2019). Database of Shear Experiments on Steel Fiber Reinforced Concrete Beams without Stirrups. Materials, 12, 917.

Li, V.C., Ward, R., Hamza, A.M. (1992) "Steel and Synthetic Fibers as Shear Reinforcement." *ACI Mat J*, 89(5): 499-508.

Li, V.C., Mishra, D.K., Naaman, A.E., Wight, J.K., LaFave, J.M., Wu, H., and Inada, Y. (1994) "On the Shear Behavior of Engineered Cementitious Composites." *Advn Cem Bas Mat*, 1994(1): 142-149.

Majdzadeh, F., Soleimani, S.M., and Banthia. N. (2006). Shear strength of reinforced concrete beams with a fiber concrete matrix. *Canadian J of Civ Eng*, 33: 726–734.

Ortiz-Navas, F., Scaroni, L., Navarro-Gregori, J., and Serna-Ros, P. (2018) *ACI SP-343: Fibre Reinforced Concrete: From Design to Structural Applications*, 91-100.

Patil, G.M., Chellapandian, M., and Prakash, S.S. (2020) "Effectiveness of Hybrid Fibers on Flexural Behavior of Concrete Beams Reinforced with Glass Fiber-Reinforced Polymer Bars." *ACI Struct J*, 117(5): 269-282.

Roesler, J.A., Altoubat, S.A., Lange, D.A., Rieder, K.A., and Ulreich, G.R. (2006) "Effect of Synthetic Fibers on Structural Behavior of Concrete Slabs-on-Ground." *ACI Mat J*, 103(1): 3-10.

Vecchio, F.J. and Collins, M.P. (1986) "The Modified Compression-Field Theory for Reinforced Concrete Elements Subjected to Shear." ACI J, 83 (2): 219–231.

Zhang, H., Calvi, P.M., Lehman, D., Kuder, K., and Roeder, C. (2020). Response of Recycled Coarse Aggregate Concrete Subjected to Pure Shear. J Struct Eng, 146(5): 04020075.